Bypass of glycan-dependent glycoprotein delivery to ERAD by up-regulated EDEM1

Efrat Ron, Marina Shenkman, Bella Groisman, Yana Izenshtein, Julia Leitman, and Gerardo Z. Lederkremer
Department of Cell Research and Immunology, George Wise Faculty of Life Sciences, Tel Aviv University, Tel Aviv 69978, Israel

ABSTRACT **Trimming of mannose residues from the N-linked oligosaccharide precursor is a stringent requirement for glycoprotein endoplasmic reticulum (ER)-associated degradation (ERAD). In this paper, we show that, surprisingly, overexpression of ER degradation–enhancing α-mannosidase-like protein 1 (EDEM1) or its up-regulation by IRE1, as occurs in the unfolded protein response, overrides this requirement and renders unnecessary the expression of ER mannosidase I. An EDEM1 deletion mutant lacking most of the carbohydrate-recognition domain also accelerated ERAD, delivering the substrate to XTP3-B and OS9. EDEM1 overexpression also accelerated the degradation of a mutant nonglycosylated substrate. Upon proteasomal inhibition, EDEM1 concentrated together with the ERAD substrate in the pericentriolar ER-derived quality control compartment (ERQC), where ER mannosidase I and ERAD machinery components are localized, including, as we show here, OS9. We suggest that a nascent glycoprotein can normally dissociate from EDEM1 and be rescued from ERAD by reentering calnexin-refolding cycles, a condition terminated by mannose trimming. At high EDEM1 levels, glycoprotein release is prevented and glycan interactions are no longer required, canceling the otherwise mandatory ERAD timing by mannose trimming and accelerating the targeting to degradation.**

Monitoring Editor
Reid Gilmore
University of Massachusetts

Received: Dec 6, 2010
Revised: Aug 25, 2011
Accepted: Sep 6, 2011

INTRODUCTION

A crucial and obligatory step in endoplasmic reticulum (ER)-associated degradation of a misfolded glycoprotein in mammalian cells is the removal of three or four α1,2-linked mannose residues from its precursor sugar chains (Frenkel *et al.*, 2003; Lederkremer and Glickman, 2005; Lederkremer, 2009; Aebi *et al.*, 2010; Hebert *et al.*, 2010). This process could be accomplished by ER mannosidase I (ERManI) by itself, through the high concentration of this enzyme in a pericentriolar subcellular compartment, the ER-derived quality control compartment (ERQC; Avezov *et al.*, 2008), but might be aided by other mannosidases (Hosokawa *et al.*, 2007; Olivari and Molinari, 2007).

An important player in this process is ER degradation–enhancing α-mannosidase-like protein 1 (EDEM1; or its yeast homologue Htm1), although the mechanism of its participation is still unclear (Kanehara *et al.*, 2007; Olivari and Molinari, 2007; Aebi *et al.*, 2010). EDEM1 was shown to bind endoplasmic reticulum-associated degradation (ERAD) substrate glycoproteins after their release from calnexin (Molinari *et al.*, 2003; Oda *et al.*, 2003), having also a chaperone-like function (Hosokawa *et al.*, 2006). Because EDEM1 is homologous to α1,2-mannosidases but does not seem to have mannosidase activity in vitro, it was initially postulated that it may act as a lectin receptor, associating with N-linked sugar chains after the mannose-trimming step (Hosokawa *et al.*, 2001; Jakob *et al.*, 2001). However, we have recently shown that EDEM1 associates with a glycoprotein substrate in the absence of the mannose-trimming activity (Groisman *et al.*, 2011). In fact, EDEM1 and its yeast homologue participate as mannosidases or cofactors in the trimming process in vivo (Olivari *et al.*, 2006; Quan *et al.*, 2008; Clerc

This article was published online ahead of print in MBoC in Press (http://www.molbiolcell.org/cgi/doi/10.1091/mbc.E10-12-0944) on September 14, 2011.

Address correspondence to: Gerardo Z. Lederkremer (gerardo@post.tau.ac.il).

Abbreviations used: ASGPR, asialoglycoprotein receptor; CRD, carbohydrate-recognition domain; EDEM1, ER degradation–enhancing α-mannosidase-like protein 1; EGFP, enhanced green fluorescent protein; ER, endoplasmic reticulum; ERAD, endoplasmic reticulum–associated degradation; ERManI, ER mannosidase I; ERQC, ER-derived quality control compartment; FCS, fetal calf serum; FITC, fluoroscein isothiocyanate; HA, hemagglutinin; HEK, human embryonic kidney; HPLC, high-performance liquid chromatography; Kif, kifunensine; Lac, lactacystin; RFP, red fluorescent protein; RT, reverse transcription; shRNA, short-hairpin RNA; UPR, unfolded protein response; XBP1s, spliced XBP1.

et al., 2009; Hosokawa *et al.*, 2010b). The lectin receptor role for the extensively trimmed species is now ascribed to OS9 and its functional homologue XTP3-B and the yeast homologue Yos9 (Hosokawa *et al.*, 2010a). We have studied the influence of elevated EDEM1, a condition that exists during the unfolded protein response (UPR), on the targeting of an ERAD substrate glycoprotein to OS9 and XTP3-B and to degradation, processes that normally depend on trimming of mannose residues. We found that EDEM1 bypasses the mannose-trimming event and delivers the glycoprotein directly to late ERAD stages.

RESULTS

When EDEM1 is overexpressed, mannose trimming and ERManI are not required for ERAD of H2a

We have used here the uncleaved precursor of the asialoglycoprotein receptor (ASGPR) H2a, a well-studied model ERAD substrate. This glycoprotein is expressed naturally in hepatocytes as a membrane precursor that undergoes efficient cleavage, producing a 35-kDa secreted form (Tolchinsky *et al.*, 1996). When H2a is expressed in other cell lines, such as NIH 3T3 or HEK 293, the membrane precursor is inefficiently cleaved and the uncleaved precursor, as well as most of the cleaved fragment, is completely retained in the ER and degraded by the ubiquitin–proteasome system (Shenkman *et al.*, 1997; Kamhi-Nesher *et al.*, 2001). ERAD of H2a requires the activity of α1,2-mannosidases (Ayalon-Soffer *et al.*, 1999; Frenkel *et al.*, 2003; Avezov *et al.*, 2008), which can be blocked with the inhibitor kifunensine (Kif), as can be seen in the pulse-chase analysis experiment of Figure 1A (compare lanes 1–2 with lanes 3–4). The lower band of the precursor in lane 1 of Figure 1A represents underglycosylated molecules (one of the three possible glycosylation sites is not occupied). The small shift of H2a to a faster mobility, as seen in the chase (Figure 1A, lane 2), is due to mannose trimming, since blocking of this trimming abrogates the shift and stabilizes H2a (Figure 1A, lanes 3–4).

Overexpression of EDEM1 (which should mimic its high levels upon UPR), accelerated the degradation of H2a (Figure 1B), as we had seen before (Groisman *et al.*, 2011). Surprisingly, upon overexpression of EDEM1, the degradation of H2a was no longer blocked by Kif (Figure 2A, compare lanes 4–6 with lanes 1–3). This is despite the shift to a slower mobility caused by Kif, which can be seen in the remaining H2a molecules (Figure 2A, compare lanes 5 and 6, and Supplemental Figure S1).

The acceleration of ERAD by EDEM1 overexpression did not require the presence of ERManI, as its knockdown, which blocks the degradation in normal conditions, as we have shown before (Avezov *et al.*, 2008), did not block it upon EDEM1 overexpression (Figure 2A, compare lanes 10–11 with lanes 7–8 and 4–5). Even upon ERManI knockdown plus cell treatment with Kif, there was no reduction in the EDEM1 acceleration of ERAD (Figure 2A, compare lanes 4–6 with lanes 10–12). In contrast to the results with EDEM1, acceleration of H2a degradation by ERManI overexpression was blocked by Kif, indicating that the effect of ERManI is dependent on mannose trimming (Figure S2). Dimers and higher oligomers of H2a can be seen in a nonreducing gel and accumulate upon Kif treatment of cells (Figure S3, lanes 1–2). EDEM1 overexpression reduced the levels of these oligomeric forms both in the absence and in the presence of Kif, suggesting that it promotes their dissociation and degradation independently of the mannose trimming. This is consistent with a chaperone activity that had been proposed for EDEM1 in dissociating aberrant misfolded protein oligomers (Hosokawa *et al.*, 2006; Olivari *et al.*, 2006).

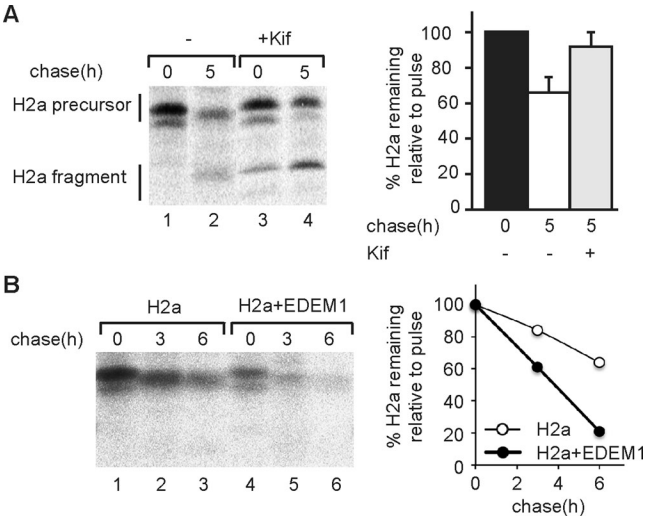

FIGURE 1: ERAD of H2a requires mannose trimming and involves EDEM1. (A) Two days after transfection of HEK 293 cells with an H2a-encoding vector, the cells were pulse-labeled for 20 min with [^{35}S] cysteine and chased for 0 or 5 h in complete medium without (lanes 1–2) or with (lanes 3–4) Kif. Kif (100 μM) was added to the cells 2 h before the labeling, and it was also present during the labeling and chase periods. After the pulse (0 h chase) or the chase periods, the cells were lysed, H2a was immunoprecipitated, and the immunoprecipitates were separated in 12% SDS–PAGE, which was followed by phosphor imaging. Bands corresponding to the H2a precursor and the naturally occurring cleaved fragment are indicated on the left. The bar graph shows percent of H2a remaining after the chase relative to the pulse, calculated from the average of phosphorimager quantitations from three independent experiments. (B) Similar to (A) but with cells transiently cotransfected with the H2a-encoding vector together with either a control GFP-encoding vector (lanes 1–3), or with an EDEM1-HA-encoding vector (lanes 4–6). The graph shows percent of H2a remaining after the chase times relative to each pulse.

We have used HEK 293 cells, although the rate of degradation of H2a is relatively slow in these cells compared with that in other cell types. However, these cells allow efficient transfection, which is needed for simultaneous expression from several plasmids combined with short-hairpin RNA (shRNA) knockdown. We wondered whether the effect of EDEM1 overexpression also occurs in other cell types and for other substrates. To test this, we expressed unassembled CD3δ, another established ERAD substrate (Fang *et al.*, 2001; Frenkel *et al.*, 2003; Kondratyev *et al.*, 2007), in NIH 3T3 cells. CD3δ degradation could be blocked with Kif. Although EDEM1 overexpression accelerated the degradation of CD3δ only modestly, it very effectively reduced the inhibition by Kif (Figure 2B).

Acceleration of ERAD caused by activation of the IRE1-dependent UPR pathway does not require mannosidase activity or ERManI

We then tested whether EDEM1 up-regulation during the UPR had a similar effect to that of direct overexpression. For this purpose, we could not use the classical UPR-inducing drugs (tunicamycin, dithiothreitol, etc.), which would directly affect the folding status of the substrate and also of EDEM1. Instead, we overexpressed the UPR sensor IRE1, a procedure that had been shown to activate the IRE1-dependent UPR pathway (Wang *et al.*, 1998; Tirasophon *et al.*, 2000), which up-regulates the expression of EDEM1. IRE1 overexpression caused a much increased degradation of H2a already during the pulse, which was not blocked by Kif (Figure 3A). The reduction of

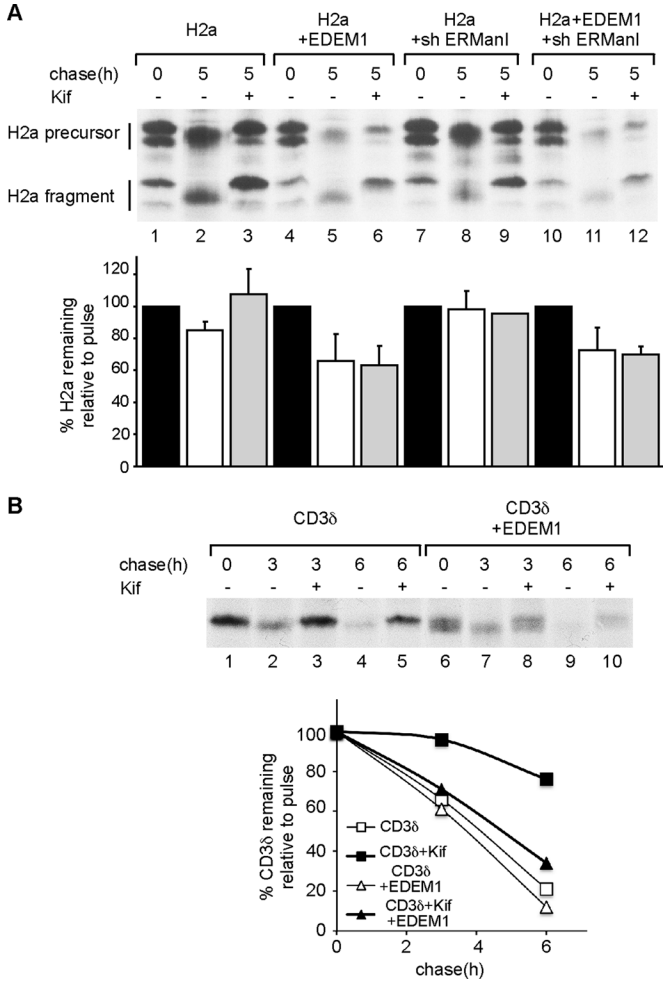

FIGURE 2: Overexpression of EDEM1 overrides the ERManI and mannose-trimming requirements for ERAD. (A) Similar to Figure 1 but performed with HEK 293 cells transiently cotransfected with the H2a-encoding vector together with either a control anti-lacZ shRNA-encoding pSUPER vector (lanes 1–3), or with the same vector encoding anti-ERManI shRNA (lanes 7–9), or with an EDEM1-HA-encoding vector (lanes 4–6), or with a combination of EDEM1-HA and anti-ERManI shRNA-encoding vectors (lanes 10–12). Cells were chased for the indicated times in complete medium in the absence or presence of Kif (100 μM; lanes 3, 6, 9, and 12). Note that here transfections were done with a higher amount of H2a-encoding vector than in Figure 1 (5 μg instead of 3 μg) to obtain higher expression and consequently slower degradation, as observed before, and thus to be able to better compare the effects of the different conditions and treatments. The bar graph shows percent of H2a remaining after chase relative to the pulse, calculated from the average of phosphorimager quantitations from three independent experiments. (B) Similar to (A) but performed with NIH 3T3 cells transiently expressing CD3δ together with either a control GFP-encoding vector (lanes 1–5) or an EDEM1-HA-encoding vector (lanes 6–10).

H2a upon IRE1 overexpression was not due to slower synthesis; protein synthesis levels remained unchanged (Figure 3B). In these conditions, there was a robust increase in the levels of endogenous EDEM1 mRNA and also at the protein level (Figure 3, C–D).

To explore whether this effect of IRE1 overexpression was mediated by EDEM1, we performed an experiment where we combined overexpression of IRE1 and knockdown of EDEM1. As shown in the preceding section, IRE1 overexpression significantly increased the degradation of H2a, which was no longer blocked by Kif (Figure 3E, lanes 4–6). EDEM1 knockdown caused a strong stabilization of H2a (Figure 3E, lanes 7–9), as we had seen before (Groisman *et al.*, 2011). Simultaneous overexpression of IRE1 and knockdown of EDEM1 partially decreased the IRE1-mediated acceleration of H2a degradation, and importantly, it restored the sensitivity to Kif (Figure 3E, compare lanes 4–6 with lanes 10–12 and graph). This result indicates that the effect of IRE1 in canceling the requirement of mannose trimming for the degradation was mediated by EDEM1. Figure 3F shows that EDEM1 up-regulation by IRE1 was significantly reduced by EDEM1 knockdown, but EDEM1 knockdown did not affect the increase in spliced XBP1 (XBP1s) mRNA levels, a direct indicator of the activation of the IRE1 branch of the UPR.

Overexpression of an EDEM1 mutant lacking the carbohydrate-recognition domain still accelerates ERAD in an ERManI-independent manner and abrogates mannose trimming dependence of substrate delivery to OS9 and XTP3B

As EDEM1 overexpression bypassed the requirement of mannose trimming for ERAD, we investigated whether its interaction with substrate glycoprotein sugar chains was at all involved in this process. For this, we aimed to overexpress a mutant EDEM1 that would not interact with sugar chains nor have any putative mannosidase activity. Several point mutants of EDEM1 had been made in conserved residues in the carbohydrate-recognition domain (CRD) that corresponds to the catalytic portion of homologous mannosidases (Olivari *et al.*, 2006; Cormier *et al.*, 2009). However, it is unclear whether any of these mutants is unable to associate to the sugar chains of the substrate; some may associate with an even stronger affinity than the wild-type protein (unpublished data). Therefore we constructed a mutant EDEM1 in which we deleted a segment encoding 156 amino acids, most of the CRD, and named it EDEM1ΔCRD (Figure 4A). EDEM1ΔCRD, expressed at a level similar to EDEM1 (Figure S4), still accelerated the degradation of H2a in an ERManI-independent manner (Figure 4B). Although no mannosidase activity was expected for EDEM1ΔCRD, it could eventually still modify in an indirect way the sugar chains of the substrate. We analyzed this possibility in a pulse-chase experiment with [2-^{3}H] mannose as a precursor and with high-performance liquid chromatography (HPLC) analysis of H2a N-linked sugar chains. Whereas overexpression of wild-type EDEM1 caused trimming of H2a N-glycans to yield mainly $Man_7GlcNAc_2$, overexpression of EDEM1ΔCRD caused no major change in the sugar chain pattern compared with the mock-transfected cells, except for a certain delay in the trimming to $Man_{5-6}GlcNAc_2$, possibly due to competition with endogenous EDEM1 or ERManI (Figure 4, C–G).

We have recently shown that mannose trimming is required for substrate delivery in cells in vivo to XTP3-B (Groisman *et al.*, 2011). In vitro, both OS9 and XTP3-B bind with high affinity to trimmed glycans and do not bind to untrimmed ones (Hosokawa *et al.*, 2008; Quan *et al.*, 2008; Yamaguchi *et al.*, 2010). We tested the effect of EDEM1ΔCRD overexpression on the coimmunoprecipitation of H2a with XTP3-B. Whereas the association was much reduced by Kif treatment of cells, overexpression of EDEM1ΔCRD canceled the requirement of mannose trimming (Figure 5, top panel, compare lanes 5–6 with lanes 7–8). This was also true for the association of H2a with OS9, though the coimmunoprecipitation was much less robust in this case (Figure 5, top panel, compare lanes 1–2 with lanes 3–4). The overexpression of EDEM1ΔCRD also reduced the overall coimmunoprecipitation of H2a with XTP3-B or OS9, possibly by nonproductive binding of EDEM1ΔCRD to the substrate.

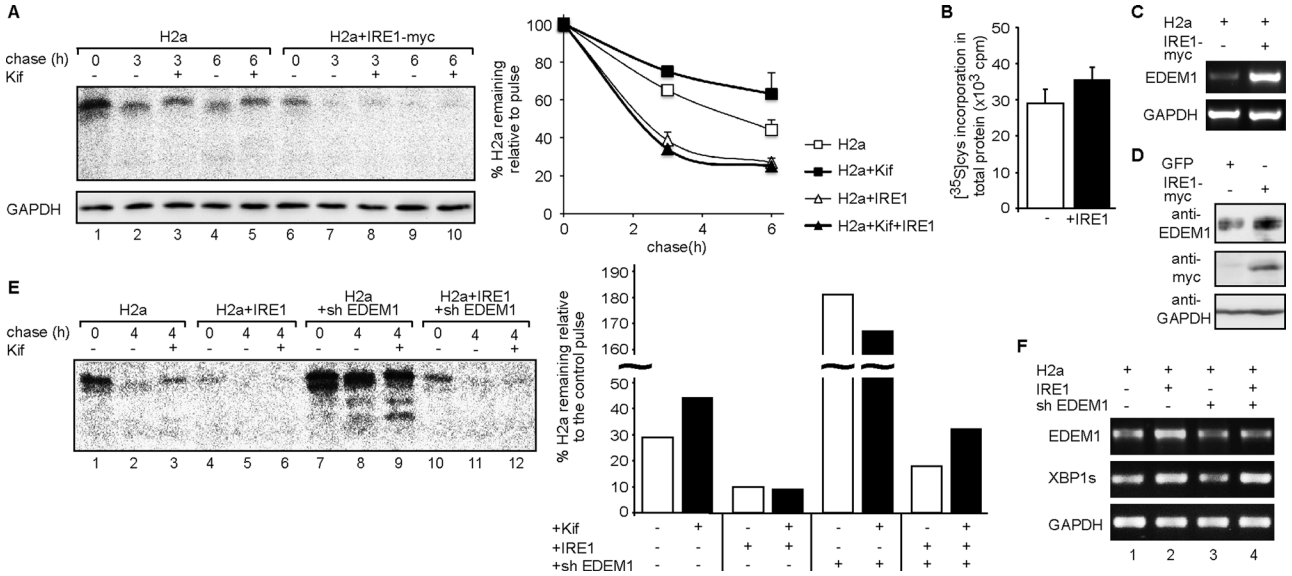

FIGURE 3: Overexpression of IRE1, simulating UPR, causes overexpression of EDEM1 and accelerates ERAD independently of mannose trimming. (A) Similar to the pulse-chase experiments in Figure 1 but performed with cells transfected with an H2a-encoding vector together with either a control GFP-encoding vector (lanes 1–5) or with a myc-tagged IRE1-encoding vector (lanes 6–10), in the presence or absence of Kif. The graph shows percent of H2a remaining after the chase relative to the pulse for each treatment, calculated from the average of three independent experiments. (B) Relative protein synthesis levels in (A) were assessed by measuring [^{35}S]Cys incorporation by total trichloroacetic acid–precipitable cpm in duplicate aliquots. (C) In parallel with (A), HEK 293 cells were transfected in the same manner and RNA was extracted 48 h posttransfection and used for RT-PCR with primers for EDEM1 mRNA (top panel) compared with GAPDH (bottom panel). (D) Cells were transfected with control GFP or with myc-tagged IRE1-encoding vectors. Two days posttransfection, cells were lysed and 10% of the lysates were run on 10% SDS–PAGE and immunoblotted with anti-myc (middle panel) or with anti-GAPDH (bottom panel). EDEM1 was immunoprecipitated from 90% of the cell lysates, run on 10% SDS–PAGE, and immunoblotted with anti-EDEM1 antibody (top panel). (E) Similar to the experiment in (A) but including samples with an anti-EDEM1 shRNA-encoding vector (lanes 7–9) and with a combination of this vector and expression of myc-tagged IRE1 (lanes 10–12). The experiment is representative of three repeat experiments. The graph shows percent of H2a remaining after the chase relative to the pulse of the cells transfected with H2a and control GFP-encoding vectors. (F) In parallel with (E), RT-PCR was done similarly to (C) but including RT-PCR with primers for spliced XBP1 mRNA.

Altogether, these results suggest the ability of EDEM1 to target substrate proteins to OS9 and XTP3-B and to ERAD in a glycan-independent manner through protein–protein interactions.

A nonglycosylated substrate can interact with OS9 and XTP3-B and can be targeted to ERAD by overexpressed EDEM1

We then tested whether H2a could in effect associate with OS9 and XTP3-B through protein–protein interactions. This was done using a nonglycosylated version of H2a we have described before, H2aΔgly, which is also an ERAD substrate. In H2aΔgly all three N-glycosylation sites are mutated (H2aΔgly; Groisman *et al.*, 2006). H2aΔgly showed significant interaction with XTP3-B and OS9 (Figure 6A). It had also been previously reported that OS9 and XTP3-B are able to interact with another nonglycosylated substrate, α1-antitrypsin NHKQQQ (Bernasconi *et al.*, 2008; Hosokawa *et al.*, 2008).

We then explored whether EDEM1 had an effect on the nonglycosylated substrate. Overexpression of EDEM1 caused a significantly accelerated degradation of H2aΔgly (Figure 6B).

These results indicate that overexpression of EDEM1 can indeed target an ERAD substrate without N-glycans, and that the substrate can associate to OS9 and XTP3-B through protein–protein interactions.

EDEM1 and OS9 localize to the ERQC and EDEM1 knockdown causes accumulation of the ERAD substrate at the ERQC

It had been observed that EDEM1 localizes mainly to vesicular structures (Zuber *et al.*, 2007). Indeed, we could see that endogenous EDEM1 appeared in a distributed punctate pattern, partially colocalizing with H2a linked to monomeric red fluorescent protein (H2aRFP; Figure 7A, top panels). To inhibit degradation of the substrate upon proteasomal inhibition, both proteins concentrated and showed a significant colocalization at the juxtanuclear ERQC compartment (Figure 7A, bottom panels). Similar results, with even higher colocalization at the ERQC upon proteasomal inhibition were seen upon overexpression of EDEM1-HA (Figure 7B). We had observed the recruitment of the ERAD substrate and components of the ERAD machinery to the ERQC upon proteasomal inhibition or UPR induction (Kondratyev *et al.*, 2007). OS9 also localized to the ERQC upon proteasomal inhibition (Figure 7C, bottom panels), but notably, OS9 also appeared concentrated in this juxtanuclear region in untreated cells (Figure 7C, top panels), similar to what we had seen for ERManI (Avezov *et al.*, 2008). Both ERManI and OS9 appear to be constitutive residents of the ERQC. They are both short-lived and OS9 was shown to be disposed of by an autophagic process (Bernasconi and Molinari, 2011).

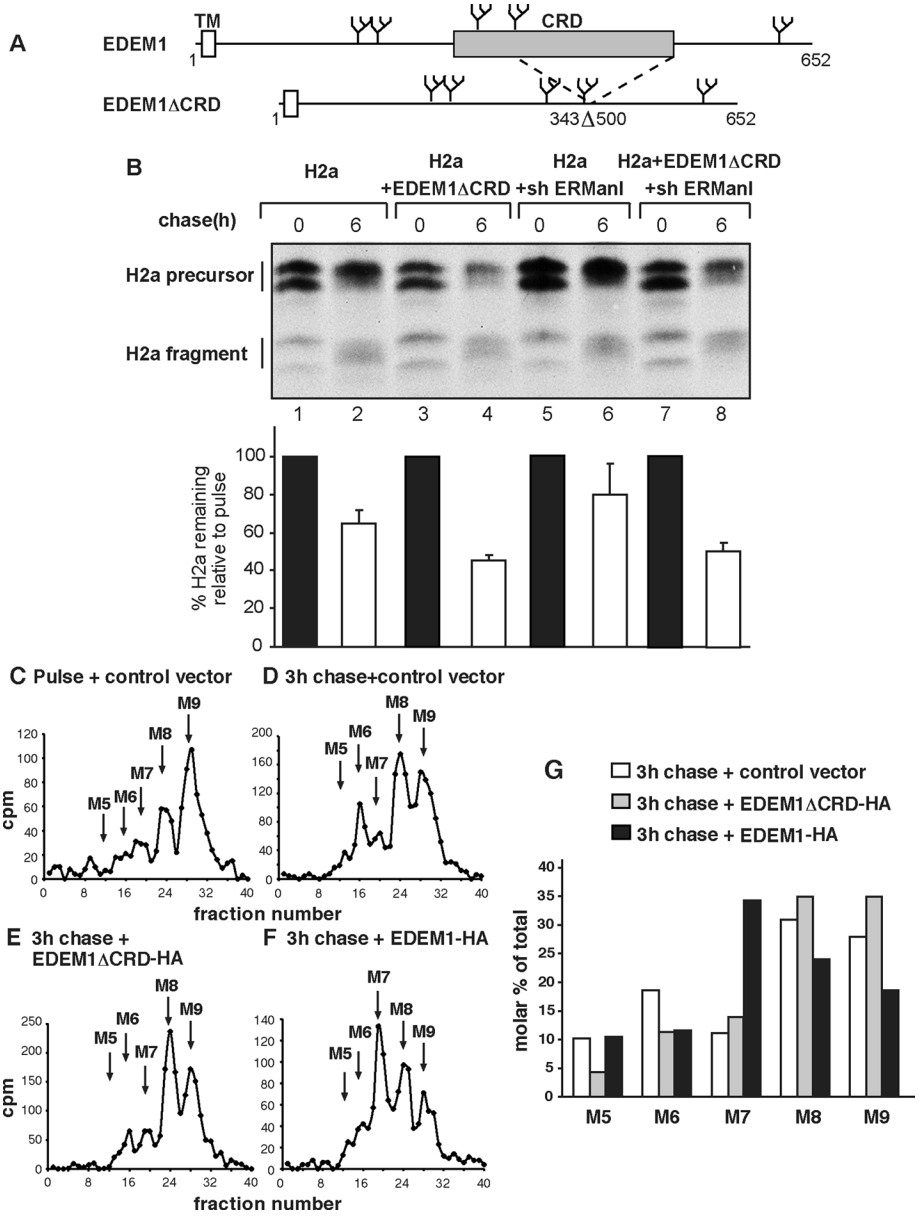

FIGURE 4: Acceleration of ERAD by overexpressed EDEM1 does not require its CRD. (A) Scheme of EDEM1 and of a mutant EDEM1 with most of its CRD deleted, but leaving its N-glycosylation sites unaffected (EDEM1ΔCRD). The white rectangle shows the transmembrane domain in EDEM1 precursor and the gray rectangle the minimal CRD. (B) HEK 293 cells were transiently cotransfected with an H2a-encoding vector together with either a control anti-lacZ shRNA-encoding pSUPER vector (lanes 1–2), or with the same vector encoding anti-ERManI shRNA (lanes 5–6), or with a vector encoding HA-tagged mutant EDEM1ΔCRD (lanes 3–4), or with a combination of EDEM1ΔCRD and anti-ERManI shRNA-encoding vectors (lanes 7–8) in conditions similar to those in Figure 1. Two days posttransfection, the cells were pulse-labeled for 20 min with [^{35}S]cysteine and chased for the indicated times, processed, and quantified as in Figure 1. (C–G) EDEM1 overexpression accelerates mannose trimming to M7, whereas EDEM1ΔCRD overexpression does not. HEK 293 cells cotransfected with an H2a-encoding vector together with either a control GFP-encoding vector (C–D), or an EDEM1ΔCRD-encoding vector (E), or an EDEM1-HA-encoding vector (F) were pulse-labeled for 1 h with [2-^{3}H]Man (0 h chase) in glucose-free medium and chased for 3 h in complete medium in the presence of 40 μM MG-132 and 25 μM ALLN. Cells were lysed and H2a was immunoprecipitated and treated with endo-β-*N*-acetylglucosaminidase H. The released N-linked oligosaccharides were separated by HPLC, fractions were counted in a beta counter, and the readout was plotted as a function of fraction number. The results shown are representative of four repeat experiments. Relative molar amounts of each oligosaccharide species were calculated based on mannose content. The percentage of each species relative to the sum of the molar amounts of all species present was then plotted (G). M5–M9 indicate migration of the standard oligosaccharides $Man_{5\text{-}9}GlcNAc$.

Accumulation of the ERAD substrate at the ERQC is dependent on ERManI and mannosidase activity. On ERManI knockdown or in the presence of inhibitors of α1,2-mannosidases, H2a distributes in a punctate pattern (Frenkel *et al.*, 2003; Avezov *et al.*, 2008). This is despite the fact that ERManI knockdown or mannose-trimming inhibitors stabilize the ERAD substrate to the same extent as proteasomal inhibition. In contrast to ERManI knockdown, anti-EDEM1 shRNA caused H2aRFP accumulation in the ERQC (Figure 7, D–F). This suggests that the mannose-trimming activity of ERManI is necessary for localization of the ERAD substrate to the ERQC, but the activity of EDEM1 is instead required for ERAD events occurring downstream of substrate accumulation in the ERQC.

DISCUSSION

Our results show that high levels of EDEM1 bypass the requirement of mannose trimming for glycoprotein ERAD. Although most of this study was done with H2a as a substrate, a similar effect on unassembled CD3δ (Figure 2) suggests a possible generality of this phenomenon. This finding has important implications, one being that the mannose-trimming "timer," which allows a time interval for newly synthesized glycoproteins to fold, will be effectively canceled upon EDEM1 up-regulation during the UPR. We can speculate that, under these conditions, nascent, still-unfolded proteins might be promptly sent to ERAD, as presumably they would not be distinguished from misfolded ones. This would clear the early secretory pathway of trafficking cargo. Another implication is that the mannose trimming of the N-glycans to $Man_{5\text{-}6}GlcNAc_2$ (Lederkremer, 2009) is not an absolute requirement for recognition or for physical movement of the glycoprotein during retrotranslocation leading to ERAD.

EDEM1 was initially postulated to be a lectin receptor, associating with N-linked sugar chains after the mannose-trimming step (Hosokawa *et al.*, 2001; Jakob *et al.*, 2001). However, we recently showed that interaction of EDEM1 with a substrate glycoprotein is not affected by inhibition of mannose trimming or knockdown of ERManI (Groisman *et al.*, 2011). This suggests that EDEM1 interacts with the substrate at an early stage in the quality control process, before the mannose-trimming step. On the other hand, if EDEM1 were required in the quality control process only at an early stage, one would expect accumulation of the substrate at this early juncture as a result of its knockdown. This is what happens with

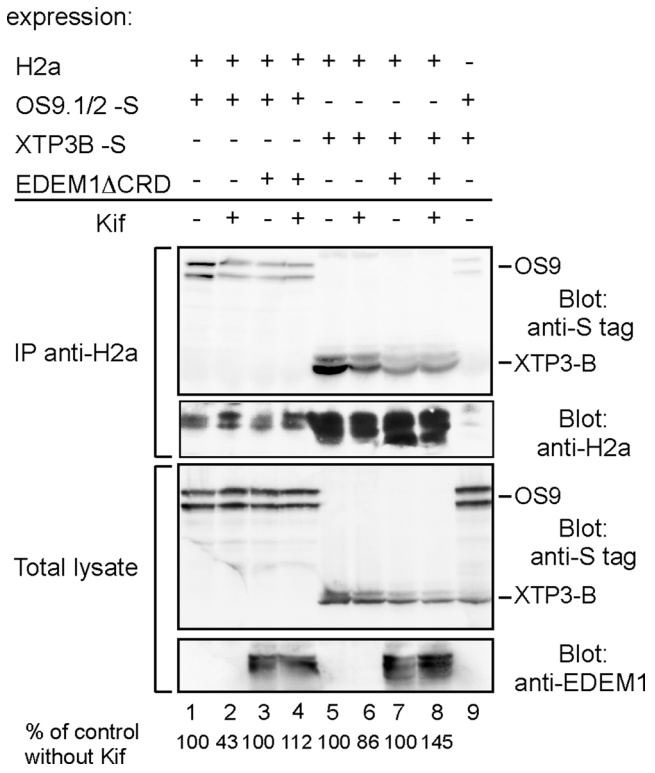

FIGURE 5: Overexpression of EDEM1ΔCRD cancels the requirement of mannose trimming for association of the ERAD substrate to XTP3-B and OS9. HEK 293 cells were cotransfected with an H2a-encoding vector together with or without an EDEM1ΔCRD-encoding vector, in the presence or absence of either S-tagged XTP3-B or a mixture of S-tagged OS9.1 and OS9.2 (S-OS9.1/2)-encoding vectors, as indicated. Lane 9 is a control without the H2a-encoding vector. Two days posttransfection, cells were incubated for 3 h in the absence/presence of 100 μM Kif. The cells were lysed and 15% of the lysates were run on 10% SDS–PAGE and immunoblotted with anti-S-tag and anti-EDEM1 antibodies (bottom panels). H2a was immunoprecipitated from 80% of the cell lysates and H2a immunoprecipitates were separated in 10% SDS–PAGE and immunoblotted with anti-H2a and anti-S-tag antibodies (top panels). The results shown are representative of three repeat experiments. Quantitations of the amounts of either S-OS9.1/2 or S-XTP3-B associated with H2a are shown at the bottom as percent of these proteins coprecipitated with H2a relative to the coprecipitation without Kif treatment.

ERManI knockdown or upon incubation of cells with a class I mannosidase inhibitor; the glycoprotein substrate accumulates in these situations in a peripheral punctate location (Frenkel *et al.*, 2003; Avezov *et al.*, 2008). In contrast, EDEM1 knockdown caused accumulation of the substrate in the ERQC (Figure 7), where OS9 and late ERAD components accumulate (Kondratyev *et al.*, 2007), suggesting that a late ERAD step is blocked. Therefore our results suggest that EDEM1 participates both in early and late steps leading to ERAD, escorting the substrate after its release from calnexin through the ERQC and to the retrotranslocation step (see model in Figure 8). At low EDEM1 levels the association and the targeting is glycan-dependent, whereas at high levels it is not. This model is consistent with the fact that EDEM1 associates with a complex containing late ERAD components like Derlin 2 and 3 (Oda *et al.*, 2006), proteins that bind to cytosolic p97 and thus could presumably participate in the retrotranslocation of the glycoprotein to the cytosol or could deliver the substrate at this stage to OS9 or XTP3-B (Christianson *et al.*, 2008; Quan *et al.*, 2008; Clerc *et al.*, 2009).

EDEM1 concentration is kept low by an autophagic process (Cali *et al.*, 2008; Bernasconi and Molinari, 2011), except upon induction of the UPR. When the UPR is induced, there is overexpression of EDEM1 (Yoshida *et al.*, 2003). IRE1 overexpression strongly up-regulated EDEM1 and led to enhanced ERAD, which was independent of mannose trimming (Figure 3). Although IRE1 also induces expression of other chaperone and ERAD genes, combined IRE1 overexpression and knockdown of EDEM1 restored the dependence of ERAD on mannose trimming, suggesting the effect was indeed mediated by EDEM1. On proteasomal inhibition, the ERAD substrate accumulates in the ERQC (Kamhi-Nesher *et al.*, 2001; Kondratyev *et al.*, 2007), colocalizing in these conditions with overexpressed EDEM1 (Figure 7). In normal conditions, most EDEM1 is seen in vesicles (Zuber *et al.*, 2007), possibly on its way from the ERQC to degradation through an autophagic pathway (Cali *et al.*, 2008). The localization of EDEM1 in the ERQC is consistent with a report that EDEM1 associates with a disulfide reductase, ERdj5 and with BiP, and that BiP dissociates from this complex at later stages (Ushioda *et al.*, 2008). Indeed, BiP is mostly excluded from the ERQC (Kamhi-Nesher *et al.*, 2001; Kondratyev *et al.*, 2007).

No mannosidase activity was found for mammalian EDEM1 in vitro, but its overexpression does accelerate mannose trimming in cells in vivo (Figure 4; Olivari *et al.*, 2006; Clerc *et al.*, 2009; Hosokawa *et al.*, 2010b). The question remains whether EDEM1 itself has mannosidase activity and needs an activator or cofactor that is only present in vivo, as was recently shown for its yeast homologue Htm1 (Gauss *et al.*, 2011), or if it accelerates mannose trimming through an indirect effect, for example, by acting itself as a cofactor or causing increased delivery to the site of trimming, the ERQC. We can conclude from our results that if EDEM1 has intrinsic mannosidase activity, this function is not needed for its role in ERAD when it is up-regulated, in contrast to the requirement of mannosidase activity for the targeting to ERAD by ERManI (Figures 2 and S2). The acceleration of ERAD of a glycoprotein by overexpression of EDEM1ΔCRD (Figure 4) and of a nonglycosylated protein by wild-type EDEM1 (Figure 6) is clear-cut evidence that EDEM1 can function in a glycan-independent manner. This is consistent with the activity seen for some point mutants of EDEM1 (Olivari *et al.*, 2006; Cormier *et al.*, 2009).

It was reported that overexpressed EDEM1 can form a complex with ERManI, inhibiting the degradation of the latter and therefore boosting its levels (Termine *et al.*, 2009). That might be another way to accelerate ERAD during the UPR, by indirectly increasing the trimming of mannose residues, as ERManI transcription is not increased in the UPR (Avezov *et al.*, 2008). Our results suggest that up-regulated EDEM1 can also directly deliver substrates to XTP-3B and OS9 and stimulate ERAD in an ERManI- and mannose trimming–independent manner. In these conditions EDEM1 and ERManI would act independently, which is consistent with the fact that overexpression of any of these proteins substantially accelerates ERAD (Figure 2; see Olivari *et al.* [2006] and Avezov *et al.* [2008]). For some substrates in *Saccharomyces cerevisiae*, it was recently observed that the EDEM1 homologue Htm1 can also act independently of Mns1, the yeast ERManI homologue, but in this case the delivery to ERAD was still dependent on the mannose-trimming activity (Hosomi *et al.*, 2010). We can speculate that the EDEM1 substrate glycoprotein may be unable to dissociate and reenter the calnexin cycle in mammalian cells at high concentration of EDEM1 (e.g., upon UPR), whereas at low EDEM1 concentration it may be released and reenter this cycle as long as less than three mannose residues have been trimmed (Figure 8). This newly acquired independence from the mannose-trimming "timer" (Lederkremer and Glickman, 2005; Lederkremer, 2009; Aebi *et al.*,

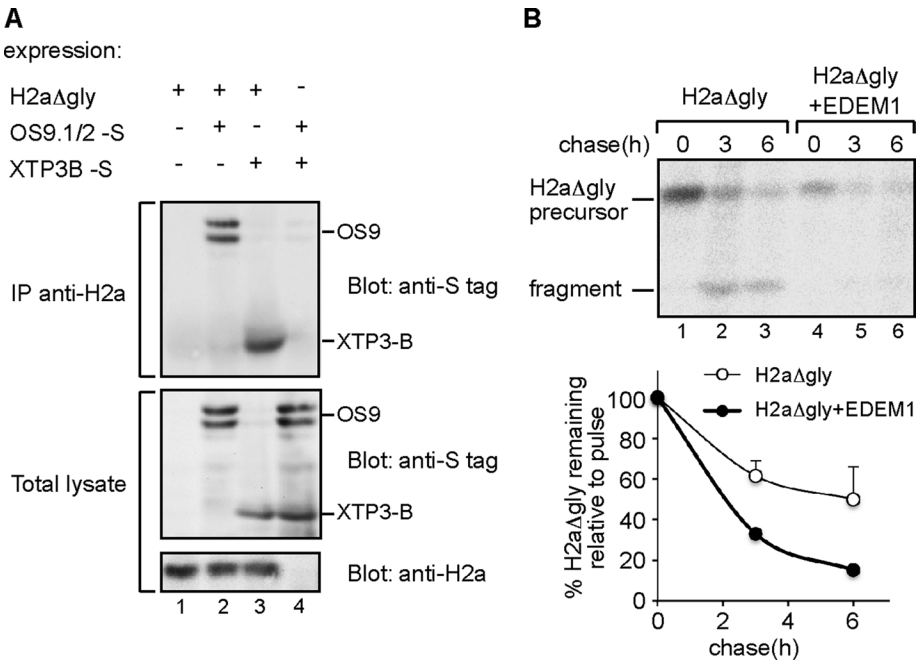

FIGURE 6: Mutant nonglycosylated H2a also associates with XTP3-B and OS9 and EDEM1 overexpression accelerates its degradation. (A) Experiment similar to the one shown in Figure 5 but analyzing coimmunoprecipitation of S-tagged XTP3-B or OS9.1/2 with a mutant H2a with its three N-glycosylation sites abrogated (H2aΔgly). (B) Pulse-chase experiment, similar to the ones in Figures 1 and 2 but with HEK 293 cells transiently cotransfected with a vector encoding H2aΔgly together with either a GFP-encoding control vector (lanes 1–3), or with an EDEM1-HA-encoding vector (lanes 4–6).

2010), which we describe here for the first time, would be one more mechanism that the cell utilizes to accelerate ERAD under the UPR, in addition to the up-regulation of ERAD machinery components (Travers *et al.*, 2000; Yoshida *et al.*, 2003), preemptive proteasomal degradation (Kang *et al.*, 2006), and the appearance of nonproteasomal degradation pathways (Shenkman *et al.*, 2007b).

MATERIALS AND METHODS

Materials

Rainbow [^{14}C]-labeled methylated protein standards were obtained from GE Healthcare (Little Chalfont, Buckinghamshire, UK). Promix cell-labeling mix ([^{35}S]Met plus [^{35}S]Cys, > 1000 Ci/mmol) and Man (D-[2-^{3}H(N)], 21 Ci/mmol) were from Perkin Elmer-Cetus (Waltham, MA). Protein A-Sepharose was from Repligen (Needham, MA). Lactacystin (Lac) and kifunensine (Kif) were from Cayman Chemicals (Ann Arbor, MI). *N*-carbobenzoxyl-leucinyl-leucinyl-leucinal (MG-132) and other common reagents were from Sigma-Aldrich (St. Louis, MO).

Plasmids and constructs

H2a subcloned in pCDNA1 was used before (Kamhi-Nesher *et al.*, 2001; Invitrogen, Carlsbad, CA). H2aΔgly in pCDNA1 was described in Groisman *et al.* (2006). A plasmid for expression of enhanced green fluorescent protein (pEGFPN1; Clontech, Mountain View, CA) or pSUPER-retro-GFP (Avezov *et al.*, 2008) were used as control vectors. The pSUPER vector carrying an shRNA for human ERManI, pSUPER encoding anti–human EDEM1 shRNA, pSUPER encoding anti–lacZ shRNA, and the pMH expression vector carrying hemagglutinin (HA)-tagged ERManI cDNA were described before (Avezov *et al.*, 2008; Groisman *et al.*, 2011). An insert for the pSUPER-retro-GFP shRNA vector with the target sequence AGATTCCACCGTCCAAGTC for human EDEM1was constructed as described in Brummelkamp *et al.* (2002). EDEM1-HA in a pCMVsport2 vector was a kind gift from K. Nagata (Kyoto University, Kyoto, Japan). To construct EDEM1ΔCRD, a region encoding most of the CRD was deleted by making two partially overlapping PCR fragments that corresponded to sequences in the 5′ half and downstream of the CRD, using the overlapping primers GGATTATTAGGCGCAACCAAGAATCCCTTCTAC and GATTCTTGGTTGCGCCTAATAATCCTGTATCGTTG and external primers at the 5′ and 3′ ends of EDEM1. These fragments were then joined in a new PCR reaction, followed by digestion with Bsp14071 and insertion into EDEM1-HA in pCMVsport2. The CRD was defined by homology with a minimal CRD of ERManI (Karaveg and Moremen, 2005). S-tagged XTP3-B, OS9.1, and OS9.2 (Christianson *et al.*, 2008) were kind gifts of R. Tyler and R. Kopito (Stanford University, Stanford, CA). H2a fused through its C terminus to monomeric red fluorescent protein (H2aRFP) and myc-tagged IRE1β in pCDNA3 were those used before (Kondratyev *et al.*, 2007).

Primers and Reverse Transcription PCR

Total cell RNA was extracted with EZ-RNA kit (Biological Industries, Beit Haemek, Israel). ReddyMix (ABgene, Epsom, UK) was used for PCR. Reverse transcription (RT) was performed with a VersoTM cDNA kit (Thermo Fisher Scientific, Barrington, IL), using a mixture of random hexamer and anchored oligo-dT primers. An aliquot (10%) of the RT product was used for PCR with the following primers: CAATGAAGGAGAAGGAGAC and CAATGTGTCCCTCTGTTGTG for EDEM1, CTTTTAACTCTGGTAAAGTGG and TTTTGGCTCCCCCCTGCAAAT for GAPDH, and TCTGCTGAGTCCGCAGCAG and GAAAAGGGAGGCTGGTAAGGAAC for spliced XBP1.

Antibodies

Rabbit polyclonal anti-H2 carboxy-terminal and anti-H2 amino-terminal antibodies were the ones used in earlier studies (Tolchinsky *et al.*, 1996; Shenkman *et al.*, 2000). R9, anti-C terminal CD3δ polyclonal was used before (Frenkel *et al.*, 2003). Rabbit polyclonal anti-EDEM1 and anti-OS9 were from Sigma and anti–S-tag from Novagen (Gibbstown, NJ). Mouse monoclonal anti-HA was from Santa Cruz Biotechnology (Santa Cruz, CA) and anti-myc was custom produced from 9E10 hybridoma. Goat anti–mouse immunoglobulin G (IgG) conjugated to FITC, and goat anti–rabbit IgG-cy2, goat anti–rabbit, and anti–mouse IgG conjugated to horseradish peroxidase (HRP) were from Jackson Labs (West Grove, PA).

Cell culture and transfections

Human embryonic kidney (HEK) 293 cells were grown in DMEM plus 10% fetal calf serum (FCS) and NIH 3T3 cells in DMEM plus 10% newborn calf serum. All cells were grown at 37°C under an atmosphere of 5% CO_2.

Transient transfection of NIH 3T3 cells was performed using the Fugene6 reagent (Roche, Basel, Switzerland) according to the kit protocol or using an MP-100 Microporator (Digital Bio Tech, Seoul,

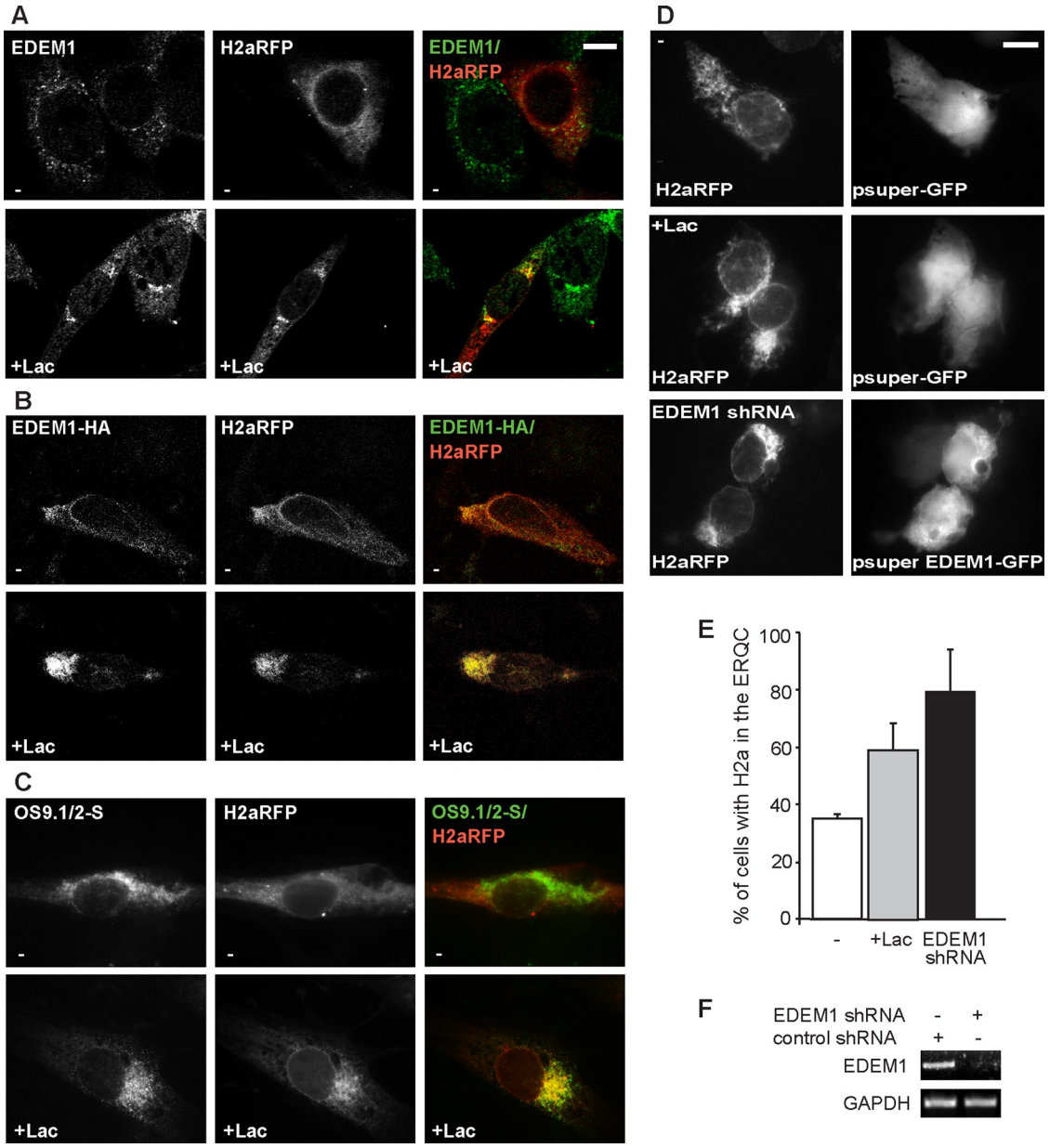

FIGURE 7: EDEM1 concentrates at the ERQC and is required for substrate accumulation at the ERQC. (A) NIH 3T3 cells were transiently transfected with a vector encoding H2aRFP. One day posttransfection, cells were incubated for 3 h without (top panels) or with (bottom panels) 25 μM lactacystin (Lac), fixed, permeabilized, reacted with rabbit anti-EDEM1 antibody and Cy2-conjugated goat anti–rabbit IgG, and visualized on an LSM confocal microscope. Representative optical slices were selected. Overlap of Cy2 with RFP appears yellow. Scale bar: 10 μm. (B) Similar to (A), except that cells were cotransfected with vectors encoding H2aRFP and EDEM1-HA and stained with mouse anti-HA and fluoroscein isothiocyanate (FITC)-conjugated goat anti–mouse IgG. (C) Similar to (B) but with cells transfected with vectors encoding S-OS9.1/2 instead of EDEM1-HA and reacted with rabbit anti-OS9 and cy2-conjugated goat anti–rabbit IgG. (D) HEK 293 cells were transfected with an H2aRFP-encoding vector together with either a control pSUPER-retro-GFP or the same vector encoding anti-EDEM1 shRNA in addition to GFP. One day posttransfection, cells were incubated for 3 h with or without 10 μM Lac, fixed, and visualized in a fluorescence microscope. (E) The bar graph shows the percent of cells with H2aRFP accumulation in the ERQC (juxtanuclear concentration) relative to the total number of cells with GFP signal under each condition, (averages of 30 cells from three independent experiments similar to the one in (D) are presented; error bars are SDs). (F) In parallel, HEK 293 cells were transfected with either pSUPER-retro-GFP or the same vector encoding anti-EDEM1 shRNA in addition to GFP; RNA was extracted 24 h posttransfection and used for RT-PCR with primers for EDEM1 mRNA compared with GAPDH.

South Korea) according to the manufacturer's instructions. Transient transfection of HEK 293 cells was done using the calcium phosphate method. The experiments were performed 24–48 h after the transfection.

[^{35}S]Cys metabolic labeling, immunoprecipitation, SDS–PAGE, and quantitation

Subconfluent (90%) cell monolayers in 60-mm dishes were labeled with [^{35}S]Cys, lysed, and immunoprecipitated with anti-H2

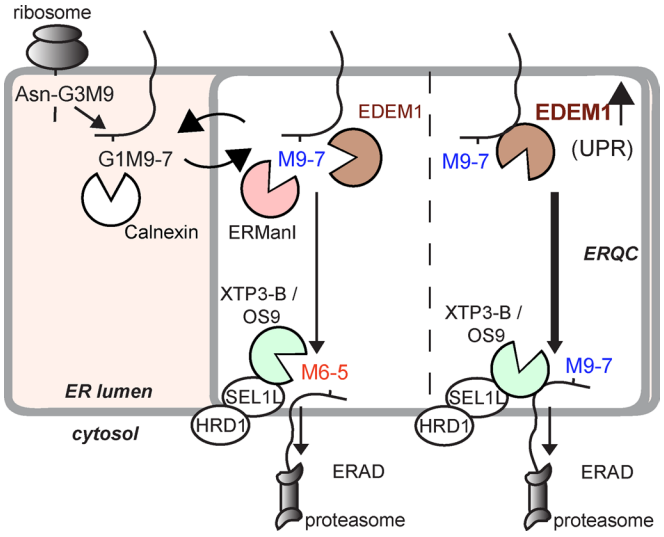

FIGURE 8: Model illustrating the bypass of the requirement for mannose trimming by up-regulated EDEM1. After cleavage from the precursor oligosaccharide of two glucose residues, the newly synthesized glycoprotein binds to calnexin (or calreticulin). The glycoprotein then moves to the ERQC, where it is deglucosylated before or upon entry and released from calnexin before associating with EDEM1. This is a crucial juncture, where the glycoprotein can be released from EDEM1 and recycled back to the peripheral ER, where it is reglucosylated before associating with calnexin. At the normally low EDEM1 concentration, the cycles repeat until a critical number of three mannose residues are excised with the intervention of ERManI (after which the glycoprotein cannot be reglucosylated), and the glycoprotein is delivered to XTP3-B or OS9 and to ERAD. However, at high concentrations (as reported in UPR conditions), EDEM1 associates to the glycoprotein through protein–protein interactions and delivers it directly to XTP3-B or OS9, bypassing the requirement for extensive mannose trimming. Triangular indentations represent sugar chain–binding domains.

antibodies, as described previously (Tolchinsky *et al.*, 1996; Shenkman *et al.*, 1997). Labeling of CD3δ with [^{35}S]Cys + [^{35}S]Met mix was done as described before (Frenkel *et al.*, 2003). Kif (100 μM) was added to the cells after the pulse labeling, except where indicated. SDS–PAGE was performed on 10% or 12% Laemmli gels. The gels were analyzed by fluorography using 20% 2,5-diphenyloxazole and were exposed to Biomax MS film using a transcreen-LE from Kodak (Vancouver, British Columbia, Canada). Quantitation was performed in a Fujifilm FLA 5100 phosphor imager (Tokyo, Japan). Relative protein synthesis levels were measured by analyzing [^{35}S]Cys incorporation in trichloroacetic acid precipitates of aliquots from labeled lysates, as described before (Shenkman *et al.*, 2007a).

[2-^{3}H]Man labeling and analysis of N-linked oligosaccharides

Subconfluent (90%) monolayers of cells in 100-mm tissue culture dishes were metabolically labeled for 60 min with 350 μCi/ml of [2-^{3}H]Man, as described previously (Frenkel *et al.*, 2003; Avezov *et al.*, 2008). Cell lysis and immunoprecipitation were performed as for the [^{35}S]-labeled samples. Endo-β-*N*-acetylglucosaminidase H treatment, high mannose N-linked oligosaccharide isolation, and separation by HPLC were as described before (Frenkel *et al.*, 2003; Avezov *et al.*, 2010) at a flow rate of 1 ml/min in acetonitrile/1% phosphoric acid (60/40 vol/vol ratio); fractions were monitored using a scintillation counter (Beckman Coulter, Brea, CA).

Coimmunoprecipitation and immunoblotting

Cell lysis was done in 1% NP-40, 50 mM Tris/HCl (pH 8), 150 mM NaCl, protease inhibitor cocktail (Roche) for 30 min on ice, and debris and nuclei were pelleted in a microfuge for 30 min at 4°C. The samples were immunoprecipitated with anti-H2a carboxy-terminal antibody and protein A-Sepharose. After overnight precipitation, the beads were washed three times with lysis buffer (diluted 1:5), which was followed by elution of the bound proteins by boiling with sample buffer containing β-mercaptoethanol at 100°C for 5 min.

Immunoblotting and detection by ECL were done as described previously (Kamhi-Nesher *et al.*, 2001), except for exposure and quantitation in a Bio-Rad ChemiDocXRS Imaging System (Bio-Rad, Hercules, CA).

Immunofluorescence microscopy

The procedures used were as described previously (Kamhi-Nesher *et al.*, 2001; Avezov *et al.*, 2008). Treatment with Lac (25 μM) of cells on coverslips was done at 37°C in a CO_2 incubator for 3–5 h. Confocal microscopy was done on a Zeiss laser-scanning confocal microscope (LSM 510; Carl Zeiss, Jena, Germany) as described before (Avezov *et al.*, 2008). For epifluorescence, digital photography was done on a Leica DMRB fluorescence microscope.

ACKNOWLEDGMENTS

We are grateful to R. Kopito and K. Nagata for reagents. The work was supported by grants from the Israel Science Foundation (1229/07) and German–Israeli Project Cooperation (DIP).

REFERENCES

Aebi M, Bernasconi R, Clerc S, Molinari M (2010). N-glycan structures: recognition and processing in the ER. Trends Biochem Sci 35, 74–82.

Avezov E, Frenkel Z, Ehrlich M, Herscovics A, Lederkremer GZ (2008). Endoplasmic reticulum (ER) mannosidase I is compartmentalized and required for *N*-glycan trimming to Man5-6GlcNAc2 in glycoprotein ER-associated degradation. Mol Biol Cell 19, 216–225.

Avezov E, Ron E, Izenshtein Y, Adan Y, Lederkremer GZ (2010). Pulse-chase analysis of N-linked sugar chains from glycoproteins in mammalian cells. J Vis Exp 38, 1899–1903.

Ayalon-Soffer M, Shenkman M, Lederkremer GZ (1999). Differential role of mannose and glucose trimming in the ER degradation of asialoglycoprotein receptor subunits. J Cell Sci 112, 3309–3318.

Bernasconi R, Molinari M (2011). ERAD and ERAD tuning: disposal of cargo and of ERAD regulators from the mammalian ER. Curr Opin Cell Biol 23, 176–183.

Bernasconi R, Pertel T, Luban J, Molinari M (2008). A dual task for the Xbp1-responsive OS-9 variants in the mammalian endoplasmic reticulum: inhibiting secretion of misfolded protein conformers and enhancing their disposal. J Biol Chem 283, 16446–16454.

Brummelkamp TR, Bernards R, Agami R (2002). A system for stable expression of short interfering RNAs in mammalian cells. Science 296, 550–553.

Cali T, Galli C, Olivari S, Molinari M (2008). Segregation and rapid turnover of EDEM1 by an autophagy-like mechanism modulates standard ERAD and folding activities. Biochem Biophys Res Commun 371, 405–410.

Christianson JC, Shaler TA, Tyler RE, Kopito RR (2008). OS-9 and GRP94 deliver mutant α1-antitrypsin to the Hrd1-SEL1L ubiquitin ligase complex for ERAD. Nat Cell Biol 10, 272–282.

Clerc S, Hirsch C, Oggier DM, Deprez P, Jakob C, Sommer T, Aebi M (2009). Htm1 protein generates the N-glycan signal for glycoprotein degradation in the endoplasmic reticulum. J Cell Biol 184, 159–172.

Cormier JH, Tamura T, Sunryd JC, Hebert DN (2009). EDEM1 recognition and delivery of misfolded proteins to the SEL1L-containing ERAD complex. Mol Cell 34, 627–633.

Fang S, Ferrone M, Yang C, Jensen JP, Tiwari S, Weissman AM (2001). The tumor autocrine motility factor receptor, gp78, is a ubiquitin protein ligase implicated in degradation from the endoplasmic reticulum. Proc Natl Acad Sci USA 98, 14422–14427.

Frenkel Z, Gregory W, Kornfeld S, Lederkremer GZ (2003). Endoplasmic reticulum-associated degradation of mammalian glycoproteins involves sugar chain trimming to Man6-5GlcNAc2. J Biol Chem 278, 34119–34124.

Gauss R, Kanehara K, Carvalho P, Ng DT, Aebi M (2011). A complex of Pdi1p and the mannosidase Htm1p initiates clearance of unfolded glycoproteins from the endoplasmic reticulum. Mol Cell 42, 782–793.

Groisman B, Avezov E, Lederkremer GZ (2006). The E3 ubiquitin ligases HRD1 and SCF^{Fbs2} recognize the protein moiety and sugar chains respectively of an ER-associated degradation substrate. Isr J Chem 46, 189–196.

Groisman B, Shenkman M, Ron E, Lederkremer GZ (2011). Mannose trimming is required for delivery of a glycoprotein from EDEM1 to XTP3-B and to late endoplasmic reticulum-associated degradation steps. J Biol Chem 286, 1292–1300.

Hebert DN, Bernasconi R, Molinari M (2010). ERAD substrates: which way out? Semin Cell Dev Biol 21, 526–532.

Hosokawa N, Kamiya Y, Kato K (2010a). The role of MRH domain-containing lectins in ERAD. Glycobiology 20, 651–660.

Hosokawa N, Tremblay LO, Sleno B, Kamiya Y, Wada I, Nagata K, Kato K, Herscovics A (2010b). EDEM1 accelerates the trimming of α1,2-linked mannose on the C branch of *N*-glycans. Glycobiology 20, 567–575.

Hosokawa N, Wada I, Hasegawa K, Yorihuzi T, Tremblay LO, Herscovics A, Nagata K (2001). A novel ER α-mannosidase-like protein accelerates ER-associated degradation. EMBO Rep 2, 415–422.

Hosokawa N, Wada I, Nagasawa K, Moriyama T, Okawa K, Nagata K (2008). Human XTP3-B forms an endoplasmic reticulum quality control scaffold with the HRD1-SEL1L ubiquitin ligase complex and BiP. J Biol Chem 283, 20914–20924.

Hosokawa N, Wada I, Natsuka Y, Nagata K (2006). EDEM accelerates ERAD by preventing aberrant dimer formation of misfolded alpha1-antitrypsin. Genes Cells 11, 465–476.

Hosokawa N, You Z, Tremblay LO, Nagata K, Herscovics A (2007). Stimulation of ERAD of misfolded null Hong Kong alpha1-antitrypsin by Golgi alpha1,2-mannosidases. Biochem Biophys Res Commun 362, 626–632.

Hosomi A, Tanabe K, Hirayama H, Kim I, Rao H, Suzuki T (2010). Identification of an Htm1 (EDEM)-dependent, Mns1-independent endoplasmic reticulum-associated degradation (ERAD) pathway in *Saccharomyces cerevisiae*: application of a novel assay for glycoprotein ERAD. J Biol Chem 285, 24324–24334.

Jakob CA, Bodmer D, Spirig U, Battig P, Marcil A, Dignard D, Bergeron JJ, Thomas DY, Aebi M (2001). Htm1p, a mannosidase-like protein, is involved in glycoprotein degradation in yeast. EMBO Rep 2, 423–430.

Kamhi-Nesher S, Shenkman M, Tolchinsky S, Fromm SV, Ehrlich R, Lederkremer GZ (2001). A novel quality control compartment derived from the endoplasmic reticulum. Mol Biol Cell 12, 1711–1723.

Kanehara K, Kawaguchi S, Ng DT (2007). The EDEM and Yos9p families of lectin-like ERAD factors. Semin Cell Dev Biol 18, 743–750.

Kang SW, Rane NS, Kim SJ, Garrison JL, Taunton J, Hegde RS (2006). Substrate-specific translocational attenuation during ER stress defines a pre-emptive quality control pathway. Cell 127, 999–1013.

Karaveg K, Moremen KW (2005). Energetics of substrate binding and catalysis by class 1 (glycosylhydrolase family 47) α-mannosidases involved in *N*-glycan processing and endoplasmic reticulum quality control. J Biol Chem 280, 29837–29848.

Kondratyev M, Avezov E, Shenkman M, Groisman B, Lederkremer GZ (2007). PERK-dependent compartmentalization of ERAD and unfolded protein response machineries during ER stress. Exp Cell Res 313, 3395–3407.

Lederkremer GZ (2009). Glycoprotein folding, quality control and ER-associated degradation. Curr Opin Struct Biol 19, 515–523.

Lederkremer GZ, Glickman MH (2005). A window of opportunity: timing protein degradation by trimming of sugars and ubiquitins. Trends Biochem Sci 30, 297–303.

Molinari M, Calanca V, Galli C, Lucca P, Paganetti P (2003). Role of EDEM in the release of misfolded glycoproteins from the calnexin cycle. Science 299, 1397–1400.

Oda Y, Hosokawa N, Wada I, Nagata K (2003). EDEM as an acceptor of terminally misfolded glycoproteins released from calnexin. Science 299, 1394–1397.

Oda Y, Okada T, Yoshida H, Kaufman RJ, Nagata K, Mori K (2006). Derlin-2 and Derlin-3 are regulated by the mammalian unfolded protein response and are required for ER-associated degradation. J Cell Biol 172, 383–393.

Olivari S, Cali T, Salo KE, Paganetti P, Ruddock LW, Molinari M (2006). EDEM1 regulates ER-associated degradation by accelerating demannosylation of folding-defective polypeptides and by inhibiting their covalent aggregation. Biochem Biophys Res Commun 349, 1278–1284.

Olivari S, Molinari M (2007). Glycoprotein folding and the role of EDEM1, EDEM2 and EDEM3 in degradation of folding-defective glycoproteins. FEBS Lett 581, 3658–3664.

Quan EM, Kamiya Y, Kamiya D, Denic V, Weibezahn J, Kato K, Weissman JS (2008). Defining the glycan destruction signal for endoplasmic reticulum-associated degradation. Mol Cell 32, 870–877.

Shenkman M, Ayalon M, Lederkremer GZ (1997). Endoplasmic reticulum quality control of asialoglycoprotein receptor H2a involves a determinant for retention and not retrieval. Proc Natl Acad Sci USA 94, 11363–11368.

Shenkman M, Ehrlich M, Lederkremer GZ (2000). Masking of an endoplasmic reticulum retention signal by its presence in the two subunits of the asialoglycoprotein receptor. J Biol Chem 275, 2845–2851.

Shenkman M, Tolchinsky S, Kondratyev M, Lederkremer GZ (2007a). Transient arrest in proteasomal degradation during inhibition of translation in the unfolded protein response. Biochem J 404, 509–516.

Shenkman M, Tolchinsky S, Lederkremer GZ (2007b). ER stress induces alternative nonproteasomal degradation of ER proteins but not of cytosolic ones. Cell Stress Chaperones 12, 373–383.

Termine DJ, Moremen KW, Sifers RN (2009). The mammalian UPR boosts glycoprotein ERAD by suppressing the proteolytic downregulation of ER mannosidase I. J Cell Sci 122, 976–984.

Tirasophon W, Lee K, Callaghan B, Welihinda A, Kaufman RJ (2000). The endoribonuclease activity of mammalian IRE1 autoregulates its mRNA and is required for the unfolded protein response. Genes Dev 14, 2725–2736.

Tolchinsky S, Yuk MH, Ayalon M, Lodish HF, Lederkremer GZ (1996). Membrane-bound versus secreted forms of human asialoglycoprotein receptor subunits—role of a juxtamembrane pentapeptide. J Biol Chem 271, 14496–14503.

Travers KJ, Patil CK, Wodicka L, Lockhart DJ, Weissman JS, Walter P (2000). Functional and genomic analyses reveal an essential coordination between the unfolded protein response and ER-associated degradation. Cell 101, 249–258.

Ushioda R, Hoseki J, Araki K, Jansen G, Thomas DY, Nagata K (2008). ERdj5 is required as a disulfide reductase for degradation of misfolded proteins in the ER. Science 321, 569–572.

Wang XZ, Harding HP, Zhang Y, Jolicoeur EM, Kuroda M, Ron D (1998). Cloning of mammalian Ire1 reveals diversity in the ER stress responses. EMBO J 17, 5708–5717.

Yamaguchi D, Hu D, Matsumoto N, Yamamoto K (2010). Human XTP3-B binds to α1-antitrypsin variant $null^{Hong\ Kong}$ via the C-terminal MRH domain in a glycan-dependent manner. Glycobiology 20, 348–355.

Yoshida H, Matsui T, Hosokawa N, Kaufman RJ, Nagata K, Mori K (2003). A time-dependent phase shift in the mammalian unfolded protein response. Dev Cell 4, 265–271.

Zuber C, Cormier JH, Guhl B, Santimaria R, Hebert DN, Roth J (2007). EDEM1 reveals a quality control vesicular transport pathway out of the endoplasmic reticulum not involving the COPII exit sites. Proc Natl Acad Sci USA 104, 4407–4412.